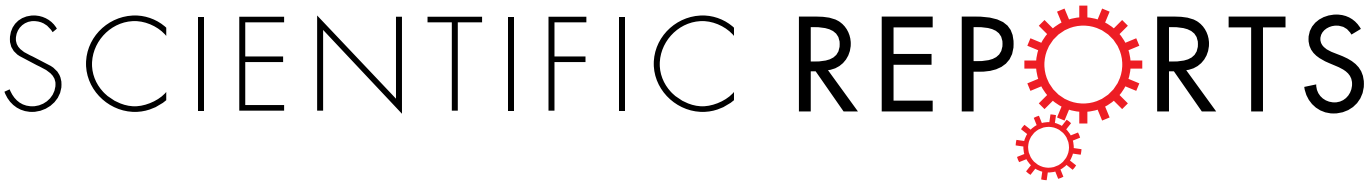

OPEN

Boreal earliest Triassic biotas elucidate globally depauperate hard substrate communities after the end-Permian mass extinction

Received: 19 May 2016
Accepted: 14 October 2016
Published: 08 November 2016

Michał Zatoń[1], Grzegorz Niedźwiedzki[2], Henning Blom[2] & Benjamin P. Kear[3]

The end-Permian mass extinction constituted the most devastating biotic crisis of the Phanerozoic. Its aftermath was characterized by harsh marine conditions incorporating volcanically induced oceanic warming, widespread anoxia and acidification. Bio-productivity accordingly experienced marked fluctuations. In particular, low palaeolatitude hard substrate communities from shallow seas fringing Western Pangaea and the Tethyan Realm were extremely impoverished, being dominated by monogeneric colonies of filter-feeding microconchid tubeworms. Here we present the first equivalent field data for Boreal hard substrate assemblages from the earliest Triassic (Induan) of East Greenland. This region bordered a discrete bio-realm situated at mid-high palaeolatitude (>30°N). Nevertheless, hard substrate biotas were compositionally identical to those from elsewhere, with microconchids encrusting *Claraia* bivalves and algal buildups on the sea floor. Biostratigraphical correlation further shows that Boreal microconchids underwent progressive tube modification and unique taxic diversification concordant with changing habitats over time. We interpret this as a post-extinction recovery and adaptive radiation sequence that mirrored coeval subequatorial faunas, and thus confirms hard substrate ecosystem depletion as a hallmark of the earliest Triassic interval globally.

The end-Permian (P-T) mass extinction 252 Ma was the most severe biotic crisis of the Phanerozoic, initiating wholesale biodiversity collapse[1–7]. Up to 90% of all marine species are estimated to have disappeared[8–11], with synchronous niche loss affecting terrestrial assemblages[12–14]. Although the underlying causes of the P-T event are not completely understood[15], a primary driver might have been massive volcanic activity within the Siberian igneous province[7,16–20]. This generated excessive emissions of thermogenic methane, CO_2 and SO_2 that cascaded oceanic warming, acidification and anoxia/euxinia with accompanying bio-productivity decline[10,16,21–28].

Ecosystem recovery after the P-T interval was seemingly protracted, but this has been reconstructed largely from the well-documented record of soft-bottom marine organisms[29–32]. In contrast, corresponding hard substrate assemblages remain enigmatic, primarily because of limited sampling. To date, the most informative fossils derive from the subequatorial shallow Panthalassic basins bordering Western Pangaea[33], and the Tethyan margin of the South China Craton[34,35]. These collectively infer disappearance of rich latest Permian encrusting benthos, and its subsequent replacement in the earliest Triassic by monogeneric colonies of microconchid tubeworms – an extinct suspension-feeding clade possibly related to 'lophophorates'[36,37]. However, the broader palaeobiogeographical continuity of these successions is speculative, especially with regard to mid-high palaeolatitude (>30°N) faunas from the Boreal Realm. These occupied a completely separate bio-region[38] and are thus crucial for establishing globally continuous patterns. Here we document the first Early Triassic Boreal hard substrate benthic assemblages from East Greenland, a remote landmass that preserves one of the most extensive P-T marine rock sections known worldwide[12,39]. Our new fossils reveal compatible microconchid predominance, but with a unique Boreal signature of morphological diversification across changing depositional settings; this not only elucidates distinctive regional endemism, but also opportunistic ecosystem expansion during the initial recovery phase after the P-T boundary.

[1]University of Silesia, Faculty of Earth Sciences, Będzińska 60, 41-200 Sosnowiec, Poland - Centre for Polar Studies KNOW (Leading National Research Centre). [2]Uppsala University, Department of Organismal Biology, Norbyvägen 18A, 752 36 Uppsala, Sweden. [3]Uppsala University, Museum of Evolution, Norbyvägen 16, 752 36 Uppsala, Sweden. Correspondence and requests for materials should be addressed to M.Z. (email: mzaton@wnoz.us.edu.pl)

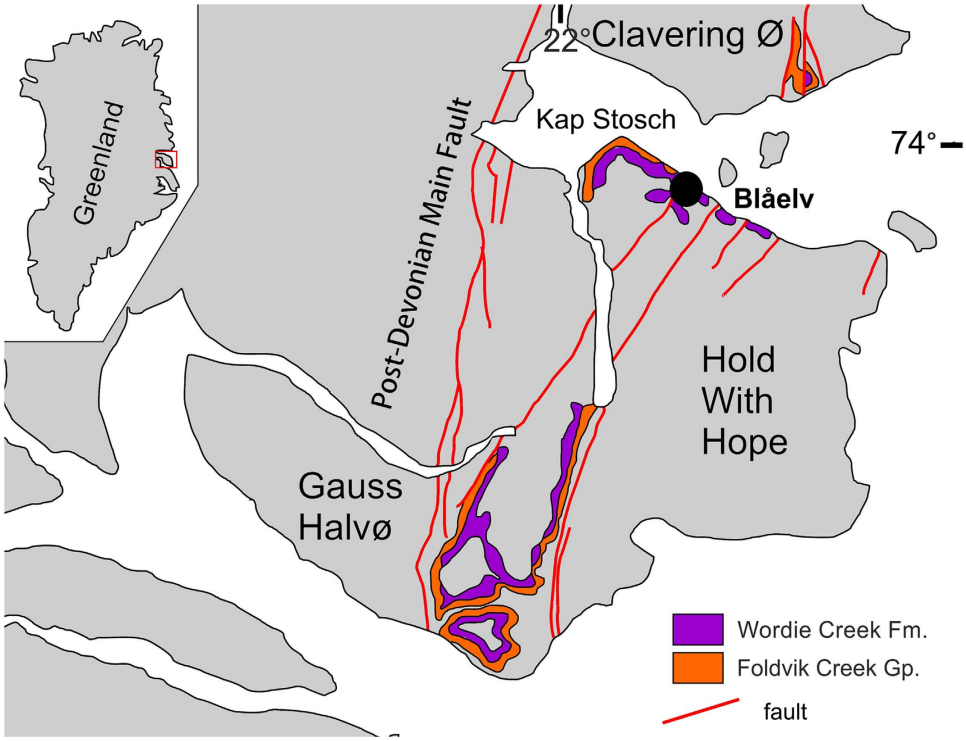

Figure 1. Locality. Map of Greenland with enlargement of the Hold with Hope peninsula showing with the Kap Stosch field site (black circle). Modified from Nielsen[42] and Bjerager *et al.*[39]. Graphics created by G.N. in *CorelDraw* 11, www.coreldraw.com.

Results

Lithostratigraphy and palaeoenvironment. We systematically collected 131 bivalve shell samples and five large rock slabs, all with encrusted microconchids, from a ~600 m transect through the Wordie Creek Formation[39–41]. This was exposed along the Blue River (Blåelv) and adjacent Stensiö Plateau at Kap Stosch on the Hold with Hope peninsula of East Greenland[42] (Fig. 1). During the latest Permian–Early Triassic, this landmass formed part of the northwestern coastal margin of Pangaea verging on the Boreal Sea. Thick siliciclastic sequences accumulated as sub-basin infills within the burgeoning rift zone between Greenland and Norway[41,43–45]. Evidence of these deposits is today preserved at Kap Stosch (Fig. 2), as well as laterally equivalent localities on Geographical Society Ø, Traill Ø, Wegener Halvø and Jameson Land[39]. The lowermost beds in the Blue River section comprise the Upper Permian (Wuchiapingian) Ravnefjeld Formation, which is unconformably overlain by a shore-face–prograding deltaic sequence containing ammonoids (*Hypophiceras triviale–Hypophiceras martini* zones: *sensu* Bjerager *et al.*[39]), and constitutes the basal horizon of the Wordie Creek Formation (Fig. 3). This earliest Triassic (Induan) unit successionally trends through marine shales and mudstones with sandy–conglomeratic turbidites in the lower–middle Griesbachian *Metophiceras subdemissum–Ophiceras commune* ammonoid zones, to mudstones and shore-face sandstones with fluvial conglomerate in the mid–upper Griesbachian to Dienerian *Wordieceras decipiens–Bukkenites rosenkrantzi* ammonoid zones[39]. Dienerian strata of the *Anodontophora breviforma–Anodontophora fassaensis* bivalve zones represent tidally-influenced paralic sandstones and overlying terrestrial red siltstones with poorly developed palaeosols, bivalves, numerous invertebrate traces, conchostracans and aquatic vertebrate remains[42,43]. Two thick sandstone bodies (SB II and SB III) also intercalate within these sediments, which are characteristically rich in fish fossils (actinopterygians and coelacanths) that provide a readily identifiable cross-referencing field zonation (Fish zones 1–5: *sensu* Nielsen[42]).

We examined five discrete fossiliferous intervals (herein numbered 1–5: Fig. 2; see also Supplementary Fig. S1) within the Wordie Creek Formation, which yielded microconchids from the *M. subdemissum*, *O. commune*, *W. decipiens* and *B. rosenkrantzi* ammonoid zones, and *A. breviforma* bivalve zone respectively (Figs 2 and 3). Lithologically these horizons comprised mudstones with abundant bivalves, and locally occurring *Archaeolithophyllum* boundstones (=red algal carbonates) grading upwards into fine-grained sandstones. *Archaeolithophyllum* algae have also been reported in the earliest Triassic deposits of Jameson Land further to the south.[46]. Dimensionally very small pyrite framboids were recovered from intervals (1) – ($M = 6.8\,\mu m$; $SD = 1.5$), (3) – ($M = 4.4\,\mu m$; $SD = 1.8$), and (4) – ($M = 5.6\,\mu m$; $SD = 1.4$). These infer dysoxic (1), to anoxic (3–4) bottom waters[23], and concur with prolific occurrences of the dysaerobic soft-substrate bivalve *Claraia*[46]. The smallest framboid diameters were derived from the *Archaeolithophyllum* boundstones of interval (3), implying microbe-enriched local anoxia. In contrast, the absence of framboids from intervals (2) and (5), coupled with prevalent crystalline pyrite, suggests periodic oxic fluctuations[23].

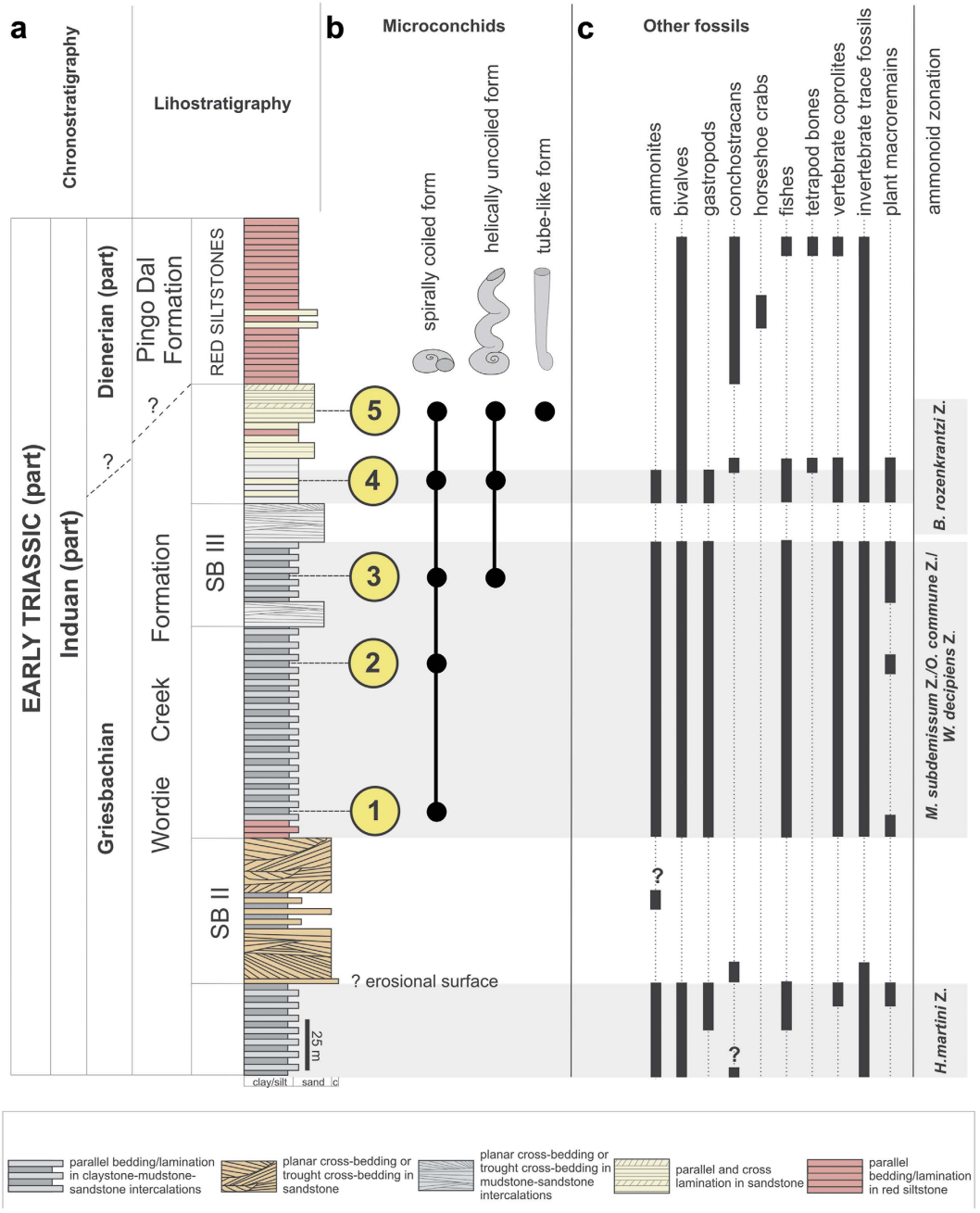

Figure 2. Lithostratigraphy and fossil content. (**a**) Schematic section of the lowermost Triassic succession at Kap Stosch with (**b**) microconchid morphotypes recovered from intervals 1–5. (**c**) Stratigraphic occurrence of associated fossils. SB II and SB III indicate major sandstone facies. Compiled and graphically drawn by G.N. in *CorelDraw* 11, www.coreldraw.com.

Microconchid assemblages. Our microconchid fossils were found attached to both *Claraia* shells and boundstones (Fig. 4). No other encrusting organisms were detected except for shallow (~1 mm deep) borings possibly attributable to the clionaid poriferan ichnite *Entobia* (Fig. 4); these were associated with a single clast from interval (3). Microconchids occurring in the boundstones infested thin calcitic sheets of *Archaeolithophyllum* (see thin section in Supplementary Fig. S2). Density of the microconchid encrustations ranged from 8–83 tubes/cm^2 across all substrates, with the most prolific coverage on *Claraia* shells in intervals (1) $M = 29.4$ tubes/cm^2, and (2) $M = 22.9$ tubes/cm^2. Colonies attached to boundstones alternatively averaged only 11.8 tubes/cm^2, but this could reflect under-sampling of the unexposed bedding planes. Abundant microconchids ($M = 29.4$ tubes/cm^2) were also scattered randomly across the mudstone layers in interval 5 (Figs 4 and 5; see also Supplementary Fig. S3), but these had likely detached (as implied by their smooth undamaged bases and lack of adhering particles: Fig. 5) from consolidated organic substrates such as algal filaments or microbial mats[47].

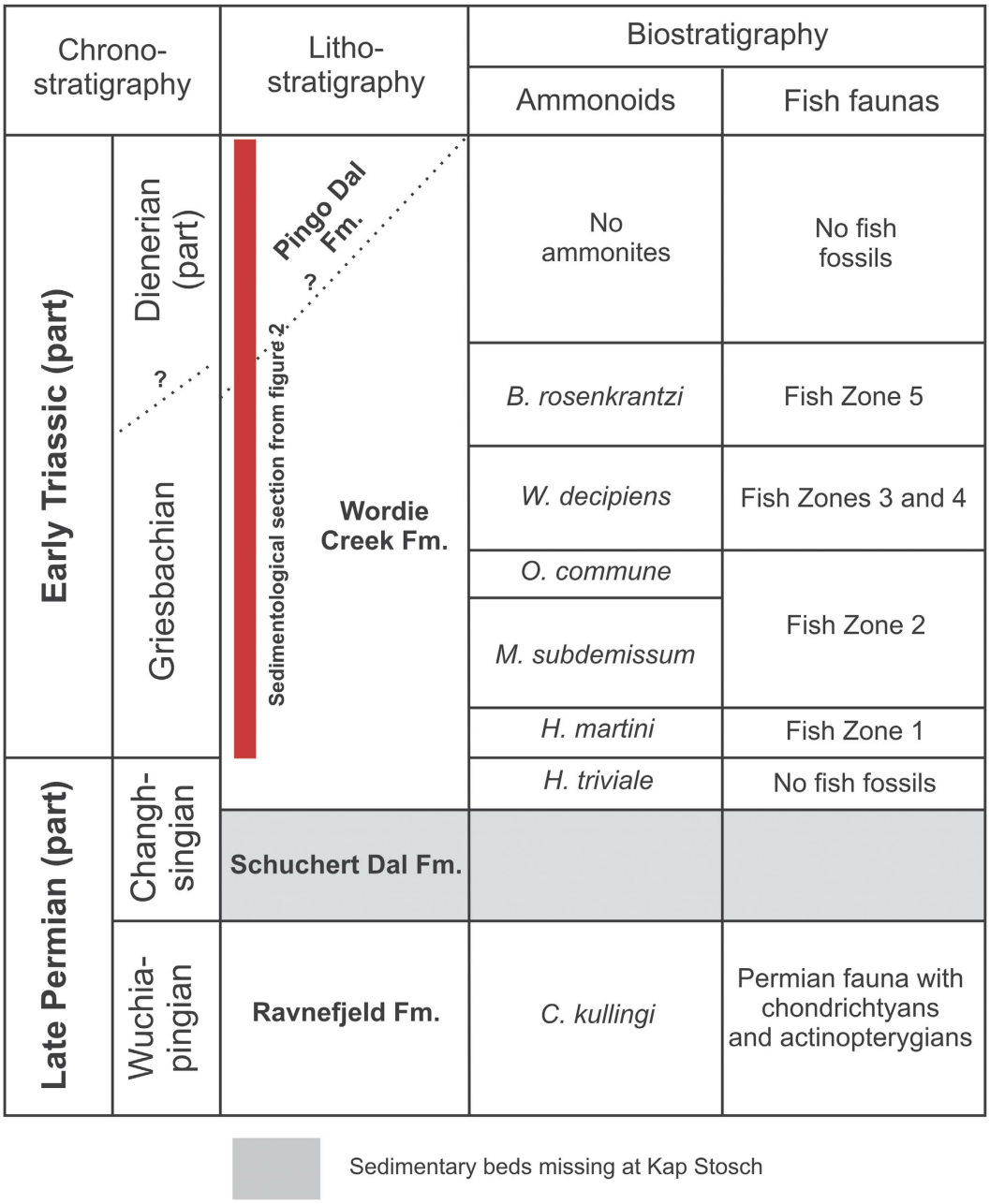

Figure 3. Biostratigraphical correlation. Upper Permian–Lower Triassic ammonoid and fish zonation[39,42,43] from Kap Stosch, East Greenland. Not depicted to scale. Compiled and graphically drawn by G.N. in *CorelDraw* 11, www.coreldraw.com.

Individual microconchid tube shapes also varied substantially between colonies, as well as across different substrates and intervals (Fig. 2). For example, those adhering to *Claraia* shells in intervals (1–5) formed squat spiral tubes, whereas those attached to algal filaments within boundstones from interval (3) displayed both spiral and helically uncoiled tubes (Fig. 5). Microconchids dispersed across mudstone layers in interval (5) were helically uncoiled and upright with a convolutional basal attachment (Fig. 5). Their external ornamentation was, nonetheless, identical with fine transverse riblets and lateral striae, accompanied by prominent punctae that penetrated the microlamellar tube structure (Supplementary Fig. S4); these features are taxonomically consistent with the genus *Microconchus* and species such as *M. valvatus*[48]. On the other hand, a unique conical tube morphotype with diminutive globular attachment area (Fig. 6) was recovered from fine-grained facies in interval (5). Its distinctive shape, coupled with unusual attachment base, surface ornamentation and tube structure comprising coarse transverse ridges and minute punctae serve to diagnose a new taxon *Spathioconchus weedoni* gen. et sp. nov. (see Supplementary Note). Structural diversity in microconchid tubes[49–51] has elsewhere been attributed to prevailing environment[52], with progressive uncoiling being an adaptation to avoid burial in accumulating sediment[49],

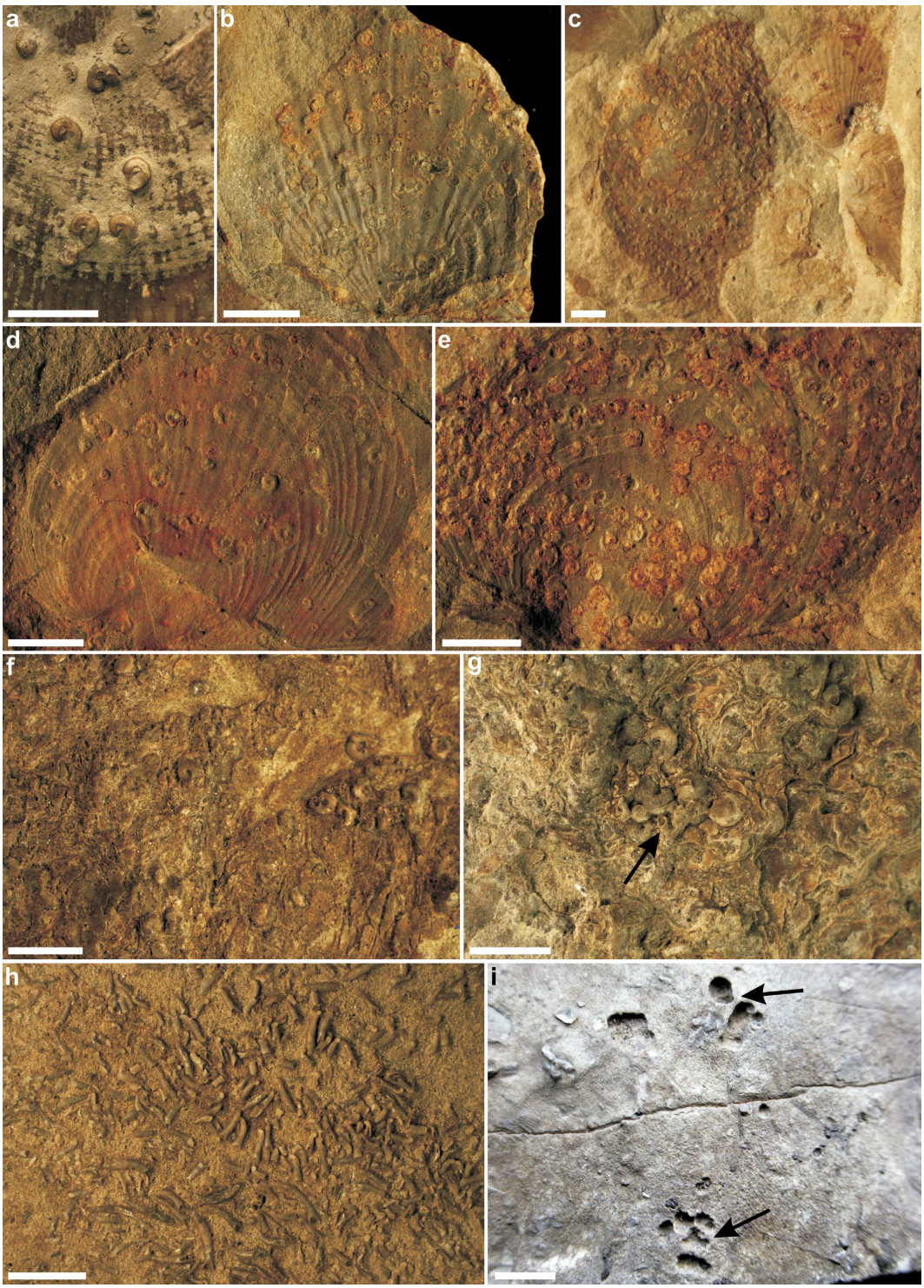

Figure 4. Triassic microconchids from Kap Stosch, East Greenland. (**a**) *Microconchus* encrusting *Claraia* shells from interval (1) (PMU 28936). (**b–e**) *Microconchus* encrusting *Claraia* shells from interval (2): (**b**) PMU 28942; (**c–e**) PMU 28940. (**f,g**) *Microconchus* encrusting *Archaeolithophyllum* boundstone from interval (3) (PMU 28954, PMU 28950); black arrow in (**g**) indicates an uncoiled tube. (**h**) Dense accumulation of *Spathioconchus weedoni* gen. et sp. nov. distributed across mudstone bedding planes from interval (5) (PMU 28962). (**i**) *Entobia*-like borings on a carbonate clast from interval 3 (PMU 28951). Scale bars 5 mm.

or overgrowth by accreting microbial mats[34]. We further interpret the reduced attachment area and peculiar conical form of *S. weedoni* as characteristics of an upright life position and densely packed colonial arrangement.

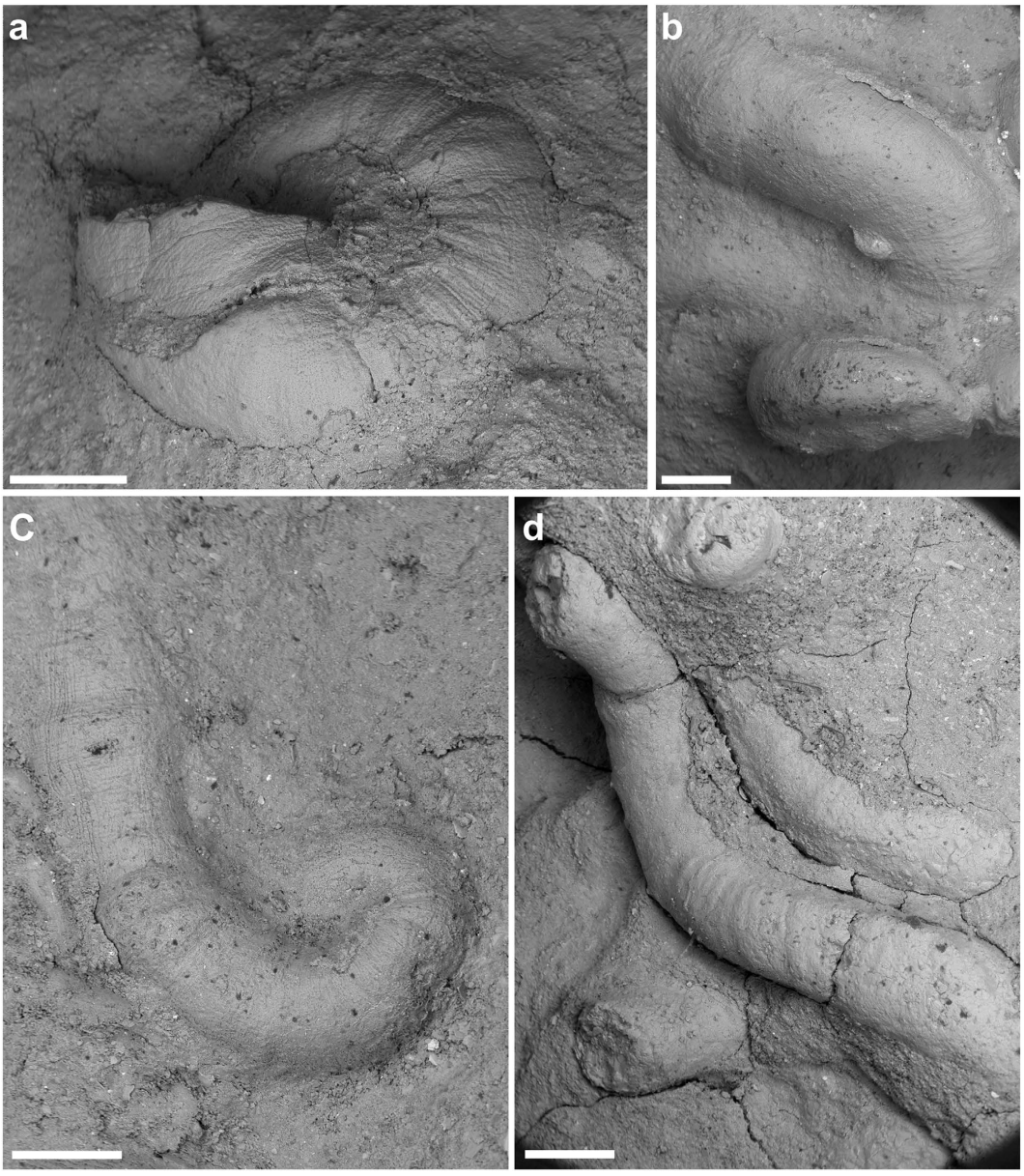

Figure 5. ESEM images of selected microconchids. (**a**) Spirally coiled *Microconchus* encrusting *Claraia* shells from interval (3) (PMU 28949). (**b,c**) Helically uncoiled *Microconchus* from interval (3) (PMU 28951). (**d**) Helically uncoiled *Microconchus* from interval (5) (PMU 28961). Scale bars 500 μm.

Discussion

The prevalence of microconchids in offshore and lower shore-face settings bordering Western Pangaea provided the original basis for positing global impoverishment of hard substrate marine ecosystems during the earliest Triassic[33]. Indeed, prolific microconchids have since been found in shallow and deep-water microbialites, on *Claraia* shells and bioclastic limestones[34,35] throughout the Tethyan Realm (Fig. 7). These mainly subequatorial palaeogeographical records are complimented here by the first equivalent Boreal occurrences, which demonstrate a coherent signature of microconchid ecosystem dominance and a near total dearth of other skeletonized encrusting organisms. Previous reports of the serpulid polychaetes *Spirorbis* and *Serpula* from Kap Stosch[53,54] and Jameson Land[12] in East Greenland can be confidently re-identified as microconchids[36]. The only other hard substrate faunal element in our samples was the *Entobia*-like ichnite, which equates to the possible phoronid boring *Talpina* from Western Pangaea[33]; however, these traces are extremely rare suggesting that endoliths, when present, constituted a minute component of the entire biotic assemblage.

In addition to their numerical abundance, both the structural and taxonomic diversity of Boreal microconchids noticeably increased over time: Griesbachian assemblages of coiled *Microconchus* being restricted to *Claraia* shells, but subsequently replaced by sympatric colonies of coiled and helically uncoiled *Microconchus* attached to *Claraia* and algal layers. Finally, conical *Spathioconchus weedoni* appeared as a novel element in mudstone

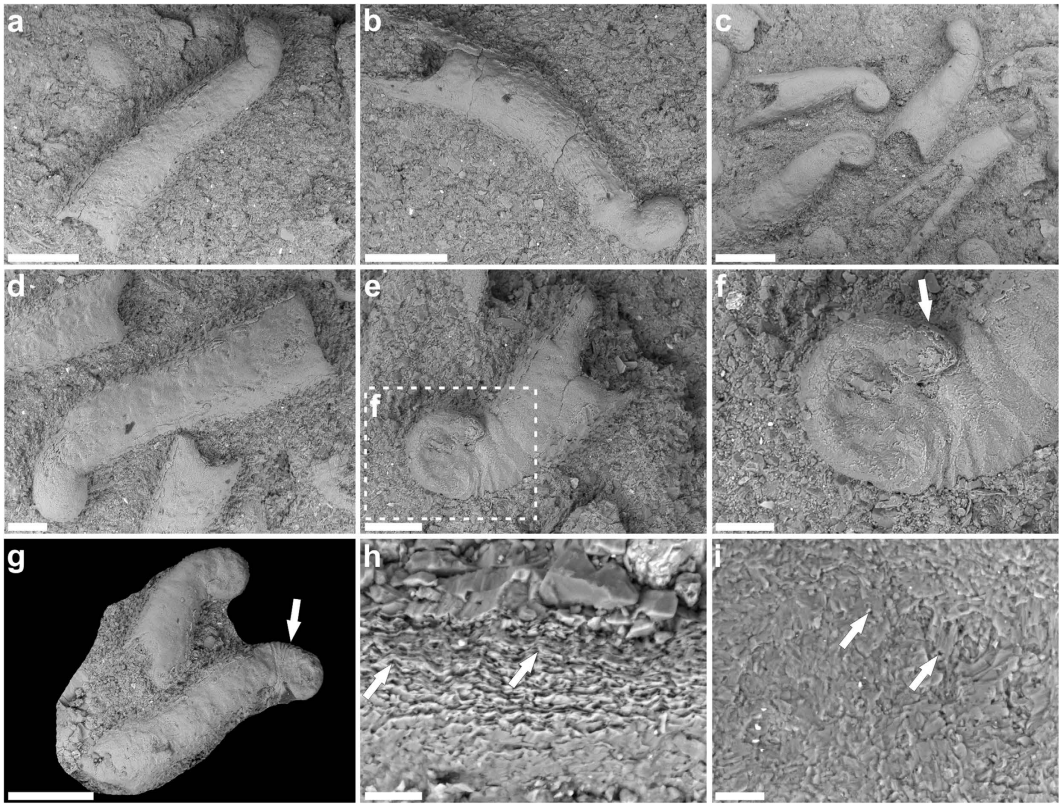

Figure 6. ***Spathioconchus weedoni*** **gen. et sp. nov.** (**a–d**) Examples showing conical tube form with small attachment base, smooth external surface and (**d**) adaperturally concave riblets. (**e,f**) Enlargement of basal attachment showing characteristic 'nucleus' (arrowed). (**g**) Holotype PMU 28962a bearing riblets at attachment base/tube border (arrowed). (**h**) Microlamellar tube structure interrupted by prominent punctae (arrowed). (**i**) Diminutive punctae (arrows) on the exfoliated tube exterior. PMU 28962. Scale bars (**a–c**,**g**) 500 μm, (**d,e**) 200 μm, (**f**) 100 μm, (**h,i**) 20 μm.

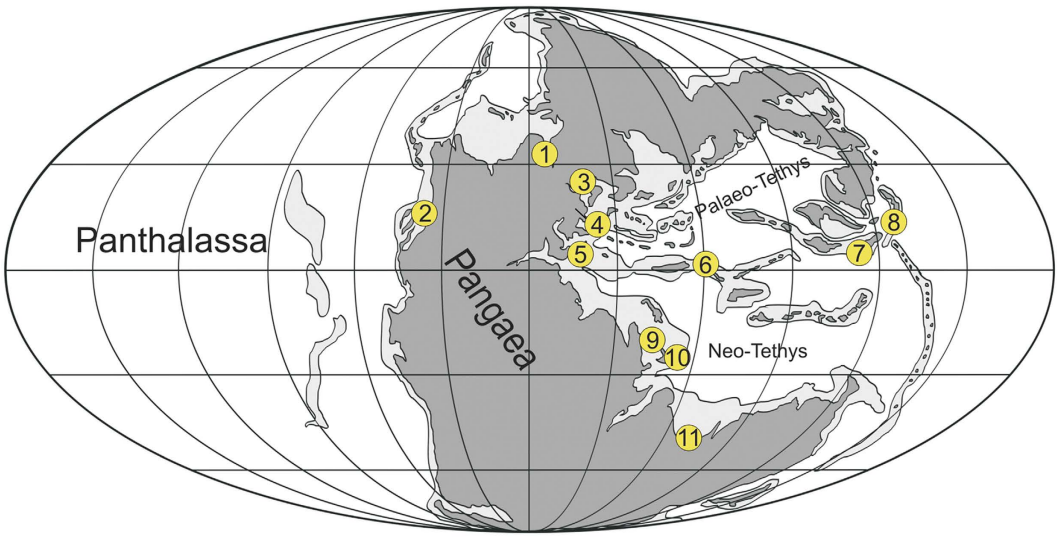

Figure 7. Palaeogeographic distribution of Early Triassic microconchids. 1. East Greenland[12,53,54]. 2. Western USA[33,60]. 3. Poland[47]. 4. Hungary[66]. 5. Italy[8,74,75]. 6. Iran[74]. 7. South China[34,35,76–78]. 8. Southwest Japan[79]. 9. Persian Gulf[80]. 10. Oman[81]. 11. Australia[82]. Palaeogeographic map from Blakey[83]. Graphics created by G.N. in *CorelDraw* 11, www.coreldraw.com.

facies from the early Dienerian onwards. This clear eco-morphological trending infers progressive adaptation and habitat expansion, incorporating an innovative dispersal into localized paralic conditions. Interestingly, Yang *et al.*[35] described similar coeval microconchid morphotypes from Griesbachian microbialites in South China. Their specimens included spiral and helically uncoiled forms resembling *Microconchus utahensis*, *Helicoconchus elongatus*, and *M. aberrans* respectively. Compatible structural diversification thus seems to have occurred in both the Boreal-Panthalassan and Tethyan realms, where microconchids paralleled stromatolites[55], inarticulate brachiopods[56], *Claraia* bivalves[4,5,57] and various foraminiferans[58] as opportunistic occupiers of benthic marine ecospace in the earliest Triassic[33–35]. By the Spathian (late Olenekian), however, bivalves and foraminiferans, together with boring suspension-feeders[33,59] had colonised hard substrates to create transient metazoan reefs; these established on multi-taxic sponge[60] and bivalve[61] frameworks during the Smithian–Spathian "coral gap"[10,11,60]. The recovery of lower tier, skeletonised biotas was therefore evidently delayed in comparison to soft-bottom communities[31,32,62], a phenomenon that we show manifested simultaneously within both low, and mid-high palaeolatitude assemblages. Certainly, some filter feeding organisms such as crinoids seem to have re-diversified earlier in the Boreal Realm (at least after the latest Induan *A. fassaensis* bivalve zone equivalent[63]), yet typical encrusters including cyclostome bryozoans and serpulid polychaetes did not fully re-establish until the Rhaetian[64]. This conspicuous underrepresentation – which is likely not taphonomic because Palaeozoic encrusters possessed similar calcitic skeletons[65] and cemented to the substrate throughout the sessile phase of their life cycle – accords with extreme fluctuations in oceanic salinity[66], de-oxygenation[9,40,67], intense weathering and run-off that are thought to have promoted widespread eutrophication and the proliferation of stromatolite-forming microbial substrates[10,11,26,68] in the absence of mat-grazing organisms[55,69]. Moreover, these markedly atypical conditions apparently favoured microconchids, which were ubiquitous across marine to brackish and even freshwater habitats[36,70,71] and readily colonized microbial/algal substrates, perhaps because of their stability and immediate supply of nutrients and oxygen[34,72]. The propagation of these environments during the earliest Triassic could therefore explain the selective survival of microconchids versus other encrusting benthos, and otherwise reflects the ecosystem homogeneity that characterised the post P-T interval on a global scale.

Methods

Our microconchid fossils were inspected using both a binocular microscope and Philips XL30 Environmental Scanning Electron Microscope (ESEM) installed at the Faculty of Earth Sciences, University of Silesia, Sosnowiec, Poland. Uncoated ESEM samples were examined with back-scattered (BSE) imaging under low vacuum conditions. Samples for pyrite framboids were thin-sectioned and assessed by ESEM. More than 50 specimens were measured and interpreted following the procedures of Wignall and Newton[73] and Bond and Wignall[23]. All fossils documented herein are housed in the Palaeontology Collection at Museum of Evolution, Uppsala University (PMU), Sweden under the registration numbers PMU 28933–PMU 28963.

References

1. Sepkoski, Jr., J. J. Patterns of Phanerozoic extinction: a perspective from global data bases in *Global events and event stratigraphy in the Phanerozoic* (ed. Walliser, O. H.) 35–51 (Springer-Verlag, 1996).
2. Bambach, R. K., Knoll, A. H. & Wang, S. C. Origination, extinction, and mass depletions of marine diversity. *Paleobiol*. **30,** 522–542 (2004).
3. Erwin, D. H. *The Great Paleozoic Crisis: Life and Death in the Permian* (Columbia University Press, New York, 1993).
4. Erwin, D. H. *Extinction. How life on Earth Nearly Ended 250 Million Years Ago.* (Princeton University Press, 2006).
5. Hallam, A. & Wignall, P. B. *Mass Extinctions and Their Aftermath* (Oxford University Press, 1997).
6. McGhee, G. R., Clapham, M. E., Sheehan, P. M., Bottjer, D. J. & Droser, M. L. A new ecological-severity ranking of major Phanerozoic biodiversity crises. *Palaeogeogr. Palaeoclimatol. Palaeoecol*. **370,** 260–270 (2013).
7. Wignall, P. B. The Worst of Times: How *Life on Earth Survived Eighty Million Years of Extinctions* (Princeton University Press, 2015).
8. Twitchett, R. J. Palaeoenvironments and faunal recovery after the end-Permian mass extinction. *Palaeogeogr. Palaeoclimatol. Palaeoecol.* **154,** 27–37 (1999).
9. Knoll, A. H., Bambach, R. K., Payne, J. L., Pruss, S. & Fischer, W. W. Paleophysiology and end-Permian mass extinction. *Earth Planet. Sci. Lett*. **256,** 295–313 (2007).
10. Algeo, T. J., Chen, Z. Q., Fraiser, M. L. & Twitchett, R. J. Terrestrial-marine teleconnections in the collapse and rebuilding of Early Triassic marine ecosystems. *Palaeogeogr. Palaeoclimatol. Palaeoecol.* **308,** 1–11 (2011).
11. Chen, Z.-Q. & Benton, M. J. The timing and pattern of biotic recovery following the end-Permian mass extinction. *Nature Geosci*. **5,** 375–383 (2012).
12. Twitchett, R. J., Looy, C. V., Morante, R., Visscher, H. & Wignall, P. B. Rapid and synchronous collapse of marine and terrestrial ecosystems during the end-Permian biotic crisis. *Geology* **29,** 351–354 (2001).
13. Benton, M., Tverdokhlebov, V. P. & Surkov, M. V. Ecosystem remodelling among vertebrates at the Permian-Triassic boundary in Russia. *Nature* **432,** 97–100 (2004).
14. Ward, P. D. *et al.* Abrupt and gradual extinction among Late Permian land vertebrates in the Karoo Basin, South Africa. *Science* **307,** 709–714 (2005).
15. Benton, M. J. & Twitchett, R. J. How to kill (almost) all life: the end-Permian extinction event. *Trends Ecol. Evol.* **18,** 358–365 (2003).
16. Wignall, P. B. Large igneous provinces and mass extinctions. *Earth Sci. Rev*. **53,** 1–33 (2001).
17. Benton, M. J. *When Life Nearly Died: The Greatest Mass Extinction of All Time* (Thames & Hudson, 2003).
18. Payne, J. L. & Kump, L. Evidence for recurrent Early Triassic massive volcanism from quantitative interpretation of carbon isotope fluctuations. *Earth Planet. Sci. Lett.* **256,** 264–277 (2007).
19. Bond, D. P. G. & Wignall, P. B. Large igneous provinces and mass extinctions: An update. *Geol. Soc. Am. Spec. Pap*. **505,** doi: 10.1130/2014.2505(02) (2014).
20. Burgess, S. D. & Bowring, S. A. High-precision geochronology confirms voluminous magmatism before, during and after Earth's most severe extinction. *Sci. Adv*. **1,** e1500470 (2015).
21. Wignall, P. B. & Twitchett, R. J. Oceanic anoxia and the end Permian mass extinction. *Science* **272,** 1155–1158 (1996).
22. Twitchett, R. J. Incompleteness of the Permian-Triassic fossil record: a consequence of productivity decline? *Geol. J*. **36,** 341–353 (2001).
23. Bond, D. P. G. & Wignall, P. B. Pyrite framboid study of marine Permian-Triassic boundary sections: a complex anoxic event and its relationship to contemporaneous mass extinction. *Geol. Soc. Am. Bull.* **122,** 1265–1279 (2010).

24. Nielsen, J. K., Shen, Y., Piasecki, S. & Stemmerik, L. No abrupt change in redox conditions caused the end-Permian marine ecosystem collapse in the East Greenland Basin. *Earth Planet. Sci. Lett.* **291,** 32–38 (2010).
25. Payne, J. L. *et al.* Calcium isotope constraints on the end-Permian mass extinction. *Proc. Nat. Acad. Sci. USA* **107,** 8543–8548 (2010).
26. Meyer, K. M., Yu, M., Jost, A. B., Kelley, B. M. & Payne, J. L. $\delta^{13}C$ evidence that high primary productivity delayed recovery from end-Permian mass extinction. *Earth Planet. Sci. Lett.* **302,** 378–384 (2011).
27. Wignall, P. B. *et al.* Ultra-Shallow marine anoxia in an Early Triassic storm-dominated clastic ramp (Spitsbergen) and the suppression of benthic radiation. *Geol. Mag.* **153,** 316–331 (2016).
28. Clarkson, M. O. *et al.* Ocean acidification and the Permo-Triassic mass extinction. *Science* **348,** 229–232 (2015).
29. Twitchett, R. J., Krystyn, L., Baud, A., Wheeley, J. R. & Richoz, S. Rapid marine recovery after the end-Permian mass extinction event in the absence of marine anoxia. *Geology* **32,** 805–808 (2004).
30. Hofmann, R., Hautmann, M., Wasmer, M. & Bucher, H. Palaeoecology of the Spathian Virgin Formation (Utah, USA) and its implications for the Early Triassic recovery. *Acta Palaeontol. Pol.* **58,** 149–173 (2013).
31. Hofmann, R., Hautmann, M. & Bucher, H. Recovery dynamics of benthic marine communities from the Lower Triassic Werfen Formation, northern Italy. *Lethaia* **48,** 474–496 (2015).
32. Hautmann, M. *et al.* Competition in slow motion: the unusual case of benthic marine communities in the wake of the end-Permian mass extinction. *Palaeontology* **58,** 871–901 (2015).
33. Fraiser, M. L. Paleoecology of secondary tierers from western Pangean tropical marine environments during the aftermath of the end-Permian mass extinction. *Palaeogeogr. Palaeoclimatol. Palaeoecol.* **308,** 181–189 (2011).
34. He, L. *et al.* Calcareous tubeworms as disaster forms after the end-Permian mass extinction in South China. *Palaios* **27,** 878–886 (2012).
35. Yang, H. *et al.* Palaeoecology of microconchids from microbialites near the Permian-Triassic boundary in South China. *Lethaia* **48,** 497–508 (2015).
36. Taylor, P. D. & Vinn, O. Convergent morphology in small spiral worm tubes ('*Spirorbis*') and its palaeoenvironmental implications. *J. Geol. Soc. London* **163,** 225–228 (2006).
37. Taylor, P. D., Vinn, O. & Wilson, M. A. Evolution of biomineralisation in 'lophophorates'. *Spec. Pap. Palaeontol.* **84,** 317–333 (2010).
38. Brayard, A. *et al.* The Early Triassic ammonoid recovery: paleoclimatic significance of diversity gradients. *Palaeogeogr. Palaeoclimatol. Palaeoecol.* **239,** 374–395 (2006).
39. Bjerager, M., Seidler, L., Stemmerik, L. & Surlyk, F. Ammonoid stratigraphy and sedimentary evolution across the Permian–Triassic boundary in East Greenland. *Geol. Mag.* **143,** 635–656 (2006).
40. Hays, L. E., Grice, K., Foster, C. B. & Summons, R. E. Biomarker and isotopic trends in a Permian–Triassic sedimentary section at Kap Stosch, Greenland. *Org. Geochem.* **43,** 67–82 (2012).
41. Sanson-Barrera, A. *et al.* Late Permian-earliest Triassic high resolution organic carbon isotope and palynofacies records from Kap Stosch (northeast Greenland). *Global Planet. Change* **133,** 149–166 (2015).
42. Nielsen, E. The Permian and Eotriassic vertebrate-bearing beds at Godthaab Gulf (East Greenland). *Medd. Grønl.* **98,** 109 pp (1935).
43. Perch-Nielsen, K., Birkenmajer, K., Birkelund, T. & Aellen, M. Revision of Triassic stratigraphy of the Scoresby Land and Jameson Land region, East Greenland. *Bull. Grønl. geol. Unders.* **109,** 51 pp (1974).
44. Surlyk, F. *et al.* The Permian of the western margin of the Greenland Sea — a future exploration target. *AAPG Bull.* **40,** 629–659 (1986).
45. Surlyk, F. Timing, style and sedimentary evolution of Late Palaeozoic–Mesozoic extensional basins of East Greenland. *Geol. Soc. Spec. Pub.* **55,** 107–125 (1990).
46. Wignall, P. B. & Twitchett, R. J. Permian–Triassic sedimentology of Jameson Land, East Greenland: incised submarine channels in an anoxic basin. *J. Geol. Soc. London* **159,** 691–703 (2002).
47. Peryt, T. M. Spirorbid-algal stromatolites. *Nature* **249,** 239–240 (1974).
48. Zatoń, M., Hagdorn, H. & Borszcz, T. Microconchids of the species *Microconchus valvatus* (Münster in Goldfuss, 1831) from the Upper Muschelkalk (Middle Triassic) of Germany. *Palaeobiodiver. Palaeoenviron.* **94,** 453–461 (2014).
49. Burchette, T. P. & Riding, R. Attached vermiform gastropods in Carboniferous marginal marine stromatolites and biostromes. *Lethaia* **10,** 17–28 (1977).
50. Zatoń, M. & Krawczyński, W. New Devonian microconchids (Tentaculita) from the Holy Cross Mountains, Poland. *J. Paleontol.* **85,** 757–769 (2011).
51. Zatoń, M. & Peck, R. L. Morphology and palaeoecology of new, non-marine microconchid tubeworm from Lower Carboniferous (Upper Mississippian) of West Virginia, USA. *Ann. Soc. Geol. Polon.* **83,** 37–50 (2013).
52. Vinn, O. Adaptive strategies in the evolution of encrusting tentaculitoid tubeworms. *Palaeogeogr. Palaeoclimatol. Palaeoecol.* **292,** 211–221 (2010).
53. Spath, L. F. Eotriassic Invertebrate Fauna of East Greenland. *Medd. Grønland* **83,** 1–90 (1930).
54. Spath, L. F. Additions to the Eotriassic invertebrate faunas of East Greenland. *Medd. Grønland* **98,** 115 pp (1935).
55. Schubert, J. K. & Bottjer, D. J. Early Triassic stromatolites as post-mass extinction disaster forms. *Geology* **20,** 883–886 (1992).
56. Rodland, D. L. & Bottjer, D. J. Biotic recovery from the end-Permian mass extinction: behaviour of the inarticulate brachiopod *Lingula* as a disaster taxon. *Palaios* **16,** 95–101 (2001).
57. Fraiser, M. L. & Bottjer, D. J. When bivalves took over the world. *Paleobiology* **33,** 397–413 (2007).
58. Song, H. *et al.* Early Triassic disaster and opportunistic foraminifers in South China. *Geol. Mag.* **153,** 298–315 (2016).
59. Zatoń, M., Taylor, P. D. & Vinn, O. Early Triassic (Spathian) post-extinction microconchids from western Pangea. *J. Paleontol.* **87,** 159–165 (2013).
60. Brayard, A. *et al.* Transient metazoan reefs in the aftermath of the end-Permian mass extinction. *Nature Geosci.* **4,** 693–697 (2011).
61. Pruss, S. B., Payne, J. L. & Bottjer, D. J. *Planucopsis* bioherms: The first metazoan buildups following the end-Permian mass extinction. *Palaios* **22,** 17–23 (2007).
62. Hautmann, M. *et al.* An unusually diverse mollusc fauna from the earliest Triassic of South China and its implications for benthic recovery after the end-Permian biotic crisis. *Geobios* **44,** 71–85 (2011).
63. Salamon, M. A., Gorzelak, P., Hanken, N.-M., Riise, H. E. & Ferré, B. Crinoids from Svalbard in the aftermath of the end-Permian mass extinction. *Pol. Polar Res.* **36,** 225–238 (2015).
64. Taylor, P. D. & Michalik, J. Cyclostome bryozoans from the late Triassic (Rhaetian) of the West Carpathians, Czechoslovakia. *Neues Jahrb. Geol. P-A* **182,** 285–302 (1991).
65. Taylor, P. D. & Wilson, M. A. Palaeoecology and evolution of marine hard substrate communities. *Earth Sci. Rev.* **62,** 1–103 (2003).
66. Foster, W. J. *et al.* Environmental controls on the post-Permian recovery of benthic, tropical marine ecosystems in western Palaeotethys (Aggtelek Karst, Hungary). *Palaeogeogr. Palaeoclimatol. Palaeoecol.* **440,** 374–394 (2015).
67. Algeo, T. J. *et al.* Plankton and productivity during the Permian-Triassic boundary crisis: an analysis of organic carbon fluxes. *Global Planet. Change* **105,** 52–67 (2013).
68. Algeo, T. J. & Twitchett, R. J. Anomalous Early Triassic sediment fluxes due to elevated weathering rates and their biological consequences. *Geology* **38,** 1023–1026 (2010).

69. Mata, S. A. & Bottjer, D. J. Microbes and mass extinctions: Paleoenvironmental distribution of microbialites during times of biotic crisis. *Geobiology* **10,** 3–24 (2011).
70. Zatoń, M., Vinn, O. & Tomescu, A. M. F. Invasion of freshwater and variable marginal marine habitats by microconchid tubeworms - an evolutionary perspective. *Geobios* **45,** 603–610 (2012).
71. Haig, D. W. *et al.* Early Triassic (early Olenekian) life in the interior of East Gondwana: mixed marine–terrestrial biota from the Kockatea Shale, Western Australia. *Palaeogeogr. Palaeoclimatol. Palaeoecol.* **417,** 511–533 (2015).
72. Chu, D. *et al.* Early Triassic wrinkle structures on land: stressed environments and oases for life. *Sci. Rep.* **5,** 10109; doi: 10.1038/srep10109 (2015).
73. Wignall, P. B. & Newton, R. Pyrite framboid diameter as a measure of oxygen deficiency in ancient mudrocks. *Am. J. Sci.* **298,** 537–552 (1998).
74. Brönnimann, P. & Zaninetti, L. On the occurrence of the serpulid *Spirorbis* Daudin,1800 (Annelida, Polychaetia, Sedentarida) in thin sections of Triassic rocks of Europe and Iran. *Riv. Ital. Paleontol. S.* **78,** 67–90 (1972).
75. Posenato, R. Survival patterns of macrobenthic marine assemblages during the end-Permian mass extinction in the western Tethys (Dolomites, Italy). *Palaeogeogr. Palaeoclimatol. Palaeoecol.* **280,** 150–167 (2009).
76. Lehrmann, D. J., Wan, Y., Wei, J., Yu, Y. & Xiao, J. Lower Triassic peritidal cyclic limestone: an example of anachronistic carbonate facies from the Great Bank of Guizhou, Nanpanjiang Basin, Guizhou Province, South China. *Palaeogeogr. Palaeoclimatol. Palaeoecol.* **173,** 103–123 (2001).
77. Lehrmann, D. J. *et al.* Permian-Triassic boundary sections from shallow-marine carbonate platforms of the Nanpanjiang Basin, South China: implications for oceanic conditions associated with the end-Permian extinction and its aftermath. *Palaios* **18,** 138–152 (2003).
78. Ezaki, Y., Liu, J., Nagano, T. & Adachi, N. Geobiological aspects of the earliest Triassic microbialites along the southern periphery of the tropical Yangtze platform: initiation and cessation of a microbial regime. *Palaios* **23,** 356–369 (2008).
79. Sano, H. & Nakashima, K. Lowermost Triassic (Griesbachian) microbial bindstone-cementstone facies, southwest Japan. *Facies* **36,** 1–24 (1997).
80. Abdolmaleki, J. & Tavakoli, V. Anachronistic facies in the Early Triassic successions of the Persian Gulf and its palaeoenvironmental reconstruction. *Palaeogeogr. Palaeoclimatol. Palaeoecol.* **446,** 213–224 (2016).
81. Baud, A. *et al.* Carbonate factory in the aftermath of the end-Permian mass extinction: Griesbachian crinoidal limestones from Oman. *Ber. Inst. Erdwiss. K.-F.-Univ. Graz* **21,** 31 (2015).
82. Thomas, B. M. *et al.* Unique marine Permian-Triassic boundary section from western Australia. *Aust. J. Earth Sci.* **51,** 423–430 (2004).
83. Blakey, R. *Global Paleogeography*. (2012). Available at: http://www2.nau.edu/rcb7/globaltext2.html (Accessed: 5th February 2016).

Acknowledgements

The Swedish Polar Research Secretariat provided field exploration funding to B.P.K. and H.B. The Faculty of Earth Sciences, University of Silesia facilitated travel and analysis of the fossils by M.Z. G.N. is financially supported by a Wallenberg Scholarship grant to Per. E. Ahlberg (Uppsala University). The Leading National Research Centre (KNOW) received by the Centre for Polar Studies for the period 2014–2018 covered publication costs for M.Z.

Author Contributions

G.N., H.B. and B.P.K. collected the fossils and lithological samples. M.Z. and G.N. analysed the data. M.Z., B.P.K., G.N. and H.B. wrote the paper.

Additional Information

Supplementary information accompanies this paper at http://www.nature.com/srep

Competing financial interests: The authors declare no competing financial interests.

How to cite this article: Zatoń, M. *et al.* Boreal earliest Triassic biotas elucidate globally depauperate hard substrate communities after the end-Permian mass extinction. *Sci. Rep.* **6**, 36345; doi: 10.1038/srep36345 (2016).

Publisher's note: Springer Nature remains neutral with regard to jurisdictional claims in published maps and institutional affiliations.